Proceedings of the 16th International Conference on Soil Mechanics and Geotechnical Engineering

doi:10.3233/978-1-61499-656-9-383

Maximum shear modulus and incrementally nonlinear soils

Module maximum de cisaillement et incrémentalement sols non-linéaires

Terence P. Holman & Richard J. Finno*
Department of Civil and Environmental Engineering
Northwestern University, Evanston, IL 60208, USA
e-mail: r-finno@northwestern.edu

ABSTRACT

Experimental results of a small strain testing program on block samples of compressible Chicago clays are presented, including bender element tests and drained axisymmetric directional stress probes employing internal measurements of axial and radial deformation and axial loads. Bender element propagation velocities and stiffness are measured during K_0 reconsolidation and creep, and are related primarily to the mean normal effective stress p′. The results of the stress probes indicate that the secant shear stiffness is directionally dependent at all strain levels between 0.001% and 0.1% under axisymmetric conditions. Because bender elements induce dispersive axisymmetric flexural waves into a soil column, the frequency of the input must be carefully selected so that the measured propagation velocity is representative of a shear wave velocity.

RÉSUMÉ

Des résultats expérimentaux d'un petit programme d'essai de contrainte sur des échantillons de bloc d'argiles compressibles de Chicago sont présentés, y compris des essais d'élément de cintreuse et des sondes directionnelles axisymmetric vidangées d'effort utilisant des mesures internes de déformation axiale et radiale et de charges axiales. Des vitesses et la rigidité de propagation d'élément de cintreuse sont mesurées pendant le reconsolidation K0 et rampent, et sont liées principalement à l'effort efficace normal moyen p '. Les résultats des sondes d'effort indiquent que le module sécant de cisaillement est directionnellement personne à charge à tous les niveaux de contrainte entre 0.001% et 0.1% dans des conditions axisymmetric. Puisque les éléments de cintreuse induisent les vagues flexural axisymmetric dispersives en colonne de sol, la fréquence de l'entrée doit être soigneusement choisie de sorte que la vitesse mesurée de propagation soit représentant d'une vitesse de vague de cisaillement.

1 INTRODUCTION

Soils are incrementally nonlinear materials for which the stiffness depends on the direction of loading and recent stress history. When developing constitutive equations to describe such behavior, it is desirable to define an upper limit for the directional stiffness at small strains. This paper presents some results of an experimental program to define the stress-strain responses of block samples of compressible Chicago clays at strain levels from 0.001% to 0.1 % under axisymmetric conditions. The experiments consisted of K_0 reconsolidation to the in-situ vertical effective stress, a creep period, and directional stress probing. Bender element tests were conducted at a number of points throughout the test to measure the propagation velocity as a function of the mean normal effective stress.

Experimental results based on measured axial and radial deformations clearly show the directionally-dependent, incrementally nonlinear response of these natural clays at strain levels greater than 0.001%. In contrast, the dynamic modulus, calculated as a function of the bender element propagation velocity, is dependent primarily on the mean normal effective stress, and does not correspond to the mechanically-measured initial shear stiffness found from any of the directional stress probes. The propagation velocities measured by bender elements are similar to those measured by seismic cone penetration tests in compressible Chicago clays at depths with the same effective stress at which the block samples were tested.

2 EXPERIMENTAL PROGRAM

The soft Chicago clay samples employed in this research program were high quality block samples obtained from the Robert H. Lurie Cancer Research Center deep excavation in downtown Chicago in December 2002 (Finno and Roboski, 2004). Three hand-cut block samples, approximately 0.3 m in each dimension (0.03 m^3 in volume) were removed from a depth of about 10.4 m below street level. Block samples are designated as LB1, LB2, or LB3. The results presented in this paper were obtained from experiments on blocks LB2 and LB3. Table 1 presents a summary of the average properties of blocks LB2 and LB3. Based on these index and stress history properties, and the sampling depth at the Lurie site, the block samples were determined to be from the Lower Blodgett till, a supraglacial deposit exhibiting erratic water contents, low OCRs, and relatively low undrained shear strengths (Chung and Finno, 1992). Comparison of the average properties in Table 1 indicates that the blocks nominally are identical.

Table 1 – Summary of average block sample properties (standard deviation in parentheses)

	Block LB2	**Block LB3**
Natural Water Content, w_n (%)	29.2 (0.5)	28.5 (0.6)
Liquid Limit, w_L (%)	38.0	37.0
Plasticity Index, I_P (%)	19.0	19.0
Void Ratio, e_0	0.82 (0.01)	0.79 (0.02)
Unit Weight, γ_t (kN/m^3)	18.9 (0.1)	19.0 (0.1)
Max. Past Pressure, σ_p' (kPa)	186	190
OCR	1.4	1.4

Eighteen triaxial specimens were hand-trimmed from the block samples. Each specimen was reconsolidated under K_0 conditions to the in-situ vertical effective stress σ_{v0}' of 134 kPa, followed by a 36 hour K_0 creep cycle. An average of 15 bender element (BE) tests was conducted during the reconsolidation of each specimen; 12 during the primary reconsolidation and 3 during creep. BE shots were typically conducted using a single-pulse sinusoidal input signal with frequency f of 2 kHz and peak-peak voltage of 14 V. Other frequencies from 500 Hz to 10 kHz were used to examine the dependence of the measured propagation velocity V_{BE} on input frequency. Wave travel times were computed using the cross correlation method (Viggiani and Atkinson, 1995). The dynamic modulus from bender elements, G_{BE}, was calculated as

$$G_{BE} = \rho V_{BE}^2 \tag{1}$$

where ρ is the total mass density of the specimen at the time of the BE shots. Implicit in the use of Eq. 1 is the assumption of plane wave propagation in an isotropic elastic cylinder.

Following the K_0 creep phase, the samples were subjected to directional stress probes under drained axisymmetric conditions. The internal deformation measurements made by the LVDTs were used to calculate raw axial and radial strain values using the measured axial gage length and sample diameter. Local measurements of axial and radial deformation were made with subminiature LVDTs mounted directly on the specimen. The linear range and accuracy of the LVDTs was ±2.5 mm and 3.6 µm, respectively. The readings of the axial LVDTs were averaged to produce a single axial deformation response, assumed to be representative of the centerline deformations within the zone of local measurement. A moving average technique was employed in order to reduce the influence of electrical noise at very small displacements and axial loads and smooth the entire data set. Groups of 100 to 250 data points were continuously averaged to produce smooth stress and strain curves centered within the raw data. Smoothed values of the local axial strain ε_a, local radial strain ε_r, and deviatoric stress q were used in Eq. 2 and 3 to calculate the local triaxial shear strain ε_s and secant shear modulus G_{sec}.

Figure 1 illustrates the stress probe directions in q-p' space. The average starting stress point for the probes was q=66 kPa and p'=90 kPa, where $q=\sigma_v'-\sigma_r'$ and $p' = (\sigma_v'+2\sigma_r')/3$. All stress probes were carried out at a stress rate $\Delta\sigma$ of 1.2 kPa/hour to minimize excess pore water pressure. Duplicate tests were conducted for the majority of the stress probes. The deviatoric axial stress was measured using an internal load cell accurate to 1.3 N. Raw deviatoric stresses were computed using the measured axial load and the current sample area, calculated using the measured radial deformation. Cell and pore pressures were measured using external differential pressure transducers. Internal stress and strain measurements were made at 5 to 20 second intervals by the data acquisition system. Triaxial shear (deviatoric) strains were calculated as

$$\varepsilon_s = \frac{2}{3}(\varepsilon_a - \varepsilon_r) \tag{2}$$

where ε_a is the axial strain and ε_r is the radial strain. Using this definition of the triaxial shear strain and assuming isotropic response, the secant shear moduli was defined as

$$G_{\sec} = \frac{\Delta q}{3\varepsilon_s} \tag{3}$$

The use of this quantity for secant stiffness, while tied to isotropic linear elasticity, is not intended to indicate reversible behavior, even at very small strains.

3 EXPERIMENTAL RESULTS

A total of 265 BE tests were conducted during the course of the K_0 reconsolidation and creep for all specimens. For each specimen, propagation velocities V_{BE} and dynamic moduli G_{BE} were plotted versus the mean normal effective stress p' in the specimen at the time of each BE test. Equation 4 was developed through power-law regression analysis of all data points from K_0 reconsolidation, not including the creep data.

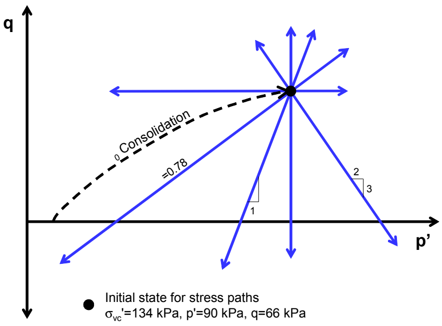

Figure 1 – Schematic diagram of drained directional stress probes

$$\frac{G_{BE}}{p_a} = 494.3\left(\frac{p'}{p_a}\right)^{0.56} \quad (R^2 = 0.84) \tag{4}$$

where p_a is atmospheric pressure. The 36 hour K_0 creep cycle caused an increase in p', which when coupled with the ageing effects, resulted in an increased V_{BE} and G_{BE}. The final G_{BE} values at the end of the creep cycle are plotted versus p' in Figure 2 for each test. The calculated value of G_{BE} ranges from 42.3 to 55.8 MPa based on V_{BE} varying between 147 m/s and 169 m/s. The mean value of G_{BE} was 50.8 MPa (SD = 3.7 MPa), and the mean value of V_{BE} was 161 m/s (SD= 6 m/s) at an average p' of 90 kPa (SD = 2.3 kPa).

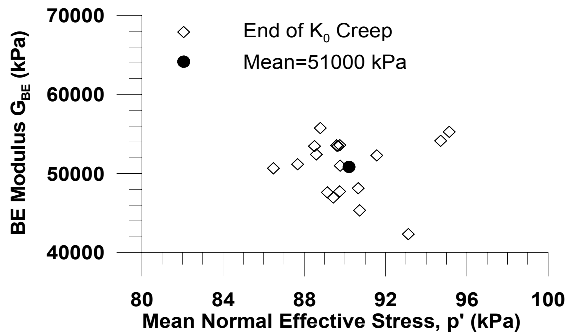

Figure 2 – Calculated G_{BE} values at end of K_0 creep

The small strain data from the directional stress probes shown in Figure 1 was processed to allow for examination of the directional shear stiffness as a function of shear strain. Figure 3 presents a plot of the secant shear modulus G_{sec} versus the triaxial shear strain ε_s for each stress probe in which the deviatoric stress q was changed. The modulus degradation curves are plotted for 0.001 %<ε_s<1.0%. The lower shear strain limit was selected because it lies between the electrical resolution of the data acquisition system (0.0001%) and the calculated accuracy of the transducers themselves (0.003%).

The secant shear moduli at 0.001% strain range from 8.5 MPa for anisotropic loading at dq/dp'=η=0.78 (sample AL) to 60.4 MPa for reduced constant mean normal stress (sample CMSE). Samples for which the deviatoric stress q was increased during the stress probe had a relatively low initial stiffness ranging from 8.5 MPa to 16.4 MPa depending on the path direction. The greatest compression-type shear modulus occurred for reduced triaxial compression (RTC). The samples undergoing extensional or unloading paths resulted in secant shear moduli values at 0.001% from 22.4 MPa to 60.4 MPa depending on path direction.

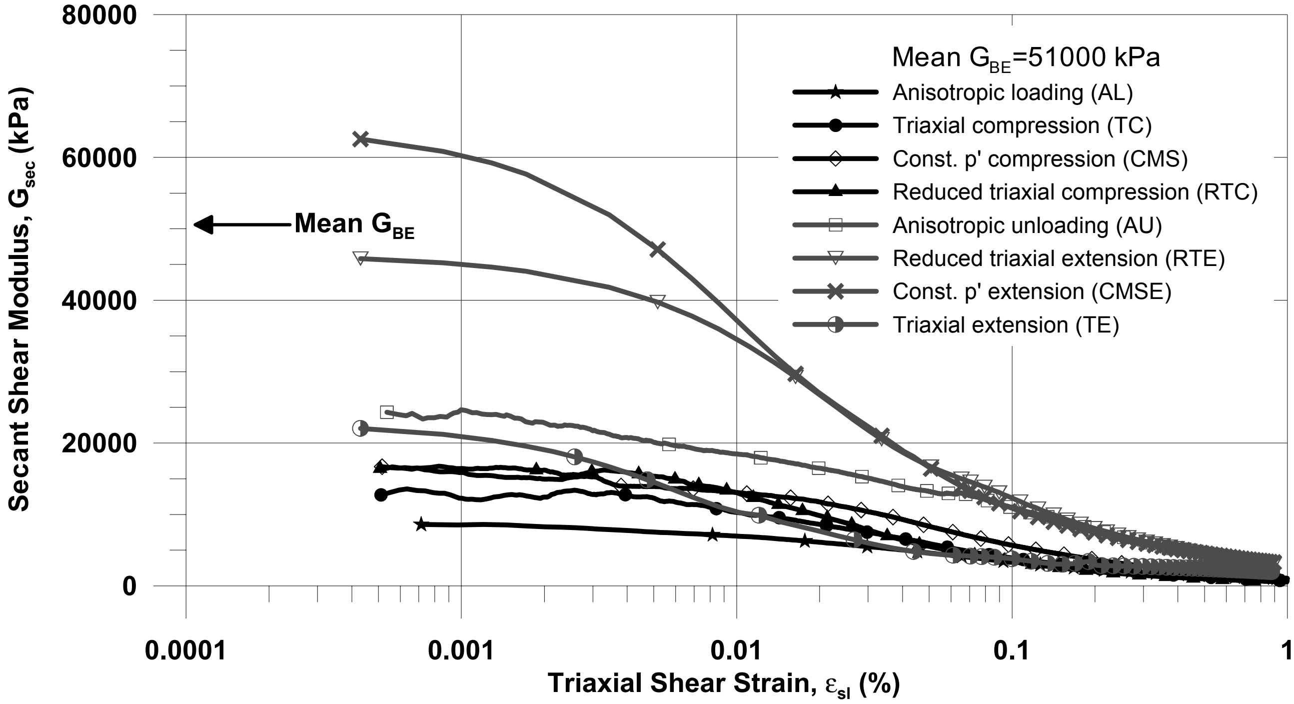

Figure 3 – Secant shear modulus degradation curves for directional stress probes

4 ANALYSIS AND INTERPRETATION

The experimental data clearly indicate that the stress-strain response of these compressible Chicago clays is directionally dependent. The stiffness of the clay generally evolves continuously and nonlinearly as a function of loading direction, recent stress history and strain level. This variability in response clearly shows these clays are incrementally nonlinear.

4.1 *Shear stiffness degradation*

The stiffness degradation behavior of the compression and extension-type stress paths are similar. The response for all paths exhibit a relatively well-defined zone of near constant stiffness for shear strains ε_s less than about 0.0001 to 0.003% followed by gradual degradation up to strains of 1.0%. The secant moduli for loading and unloading directions asymptotically approach constant values at strains greater than 1%, a reasonable trend considering that at these strain levels, soft, lightly overconsolidated clays are close to failure.

The directional shear stiffness behavior and the effects of recent stress history can also be observed in the degradation data in Figure 3. According to Atkinson et al. (1990) the recent stress history of a soil element has a very strong influence on the stiffness, with the stiffest response associated with a complete reversal of previous stress path direction. Figure 4 summarizes the values $G_{0.001}$ along each stress path in q-p' space and graphically depicts the length and direction of the stress vector causing mobilization of $G_{0.001}$. The anisotropic loading test AL most closely matches the continued loading direction of the K_0 consolidation history (i.e. the recent stress history), with an average η=0.74, and results in an initial secant shear stiffness of 8.5 MPa. $G_{0.001}$ for AU is 24.5 MPa, approximately 3 times greater than for AL, the path 180 degrees opposite. While this difference is indeed large, the greatest mobilized secant shear stiffness occurred for stress path CMSE which is approximately 230 degrees counterclockwise from path AL. Based on this data, the shear stiffness is strongly directionally dependent.

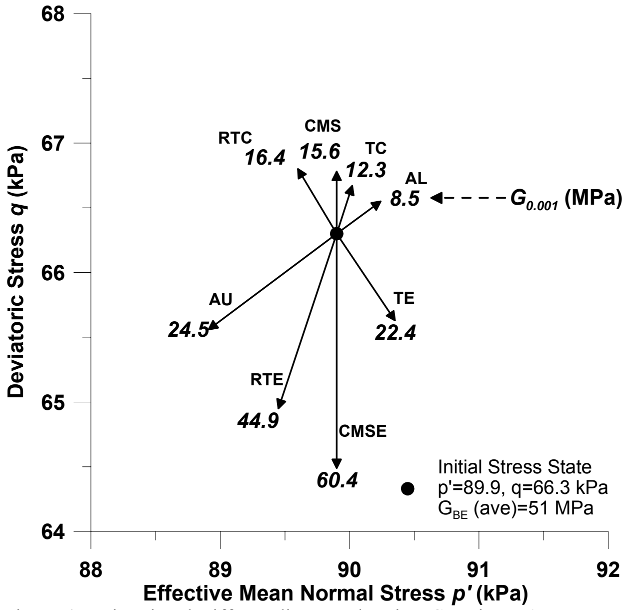

Figure 4 – Directional stiffness diagram showing $G_{0.001}$ in q-p' space

Unlike the $G_{0.001}$ from the directional stress probes, the dynamic modulus G_{BE} determined during the stress probe portions of the tests reported herein is primarily dependent on the mean normal effective stress p' (Holman 2005). G_{BE} is commonly assumed to represent the maximum shear modulus G_{max} at very small strains between 0.0001 and 0.001% (Dyvik and Madshus, 1985), similar to the assumed strain levels for field geophysical testing such as seismic cone penetration (SCPT). As mentioned previously, the mean V_{BE} was 161 m/s, resulting in an average G_{BE} value of 51 MPa. SCPT studies at a Chicago area project site with very similar subsurface conditions and stress history indicated that the in-situ shear wave velocity V_s at the same vertical effective stress as the block samples ranged from 170 to 180 m/s (Mayne 2003). The relatively small difference between the field and laboratory propagation velocities, 5 to 10%, normally would suggest that the field and laboratory stiffness are very similar. Examination of the very small strain moduli G_{BE}

in Figure 1 and the initial secant moduli $G_{0.001}$ for the directional stress probes in Figure 3 indicates that G_{BE} is approximately equal to that defined by paths RTE and CMSE, or the maximum values measures in the stress probe experiments.

If G_{BE} represents an elastic modulus, then inducing unloading paths would be a reasonable way to measure this value in a mechanical test. Given the directionality of the $G_{0.001}$ responses, a path like CMSE wherein unloading is accomplished at constant effective stress would be a consistent approach to obtain an "elastic" modulus that corresponds to a bender element loading where small shear stresses are applied to the top of a cylindrical soil specimen.

4.2 *Comments on bender element results*

Conventional methods of interpreting bender element results assume that the propagated wave is a plane wave and that the soil medium through which it travels is an isotropic elastic cylinder. The propagation velocity V_{BE} is assumed to be the shear wave velocity, V_s, and the dynamic modulus, G_{BE}, is assumed to be the maximum shear modulus, G_{max}. In this case, Eq. 1 is strictly valid if one-dimensional wave propagation is appropriate. In general, the presence of finite boundaries causes the specimen to act as a waveguide by virtue of the wave reflections occurring on the boundaries. This introduces complications into the simplified analysis represented by Eq. 1. More generally, the perturbation caused by the transmitter bender element induces antisymmetric flexural waves to the specimen. These waves are dispersive, meaning that the group velocity V_g of each branch is frequency-dependent (Achenbach, 1973).

Wang (2004) presented numerical solutions for the nondimensional frequency Ω versus normalized group velocity V^* for flexural waves for both free-standing and embedded cylinders (Wang, 2004). Achenbach (1973) defined the nondimensional frequency Ω as

$$\Omega = \frac{\omega r}{V_s} = \frac{2\pi f r}{V_s} \tag{5}$$

where ω is the angular frequency, f is the frequency, r is the cylinder radius, and V_s is the true shear wave velocity (i.e. the distortional body wave which propagates through an isotropic infinite elastic medium). The normalized group velocity, V^*, is defined as V_g / V_s. Following Achenbach (1973), the theoretical curve for the first branch of the first flexural mode, F(1,1), is plotted in Figure 5 in Ω - V^* space for Poisson's ratio, ν, of 0.1. Bender element data from two samples, obtained at input frequencies ranging from 500 Hz to 10 kHz and various p' values during reconsolidation were normalized and plotted on Figure 5. Parametric studies were carried out to estimate the shear wave velocity V_s with which to normalize the calculated V_{BE} values. The data points span Ω values from 0.75 to 22 and V^* values from 0.72 to 1.0.

The fit of the experimental data points about the theoretical curve clearly indicates that V_{BE} (and subsequently G_{BE}) at a given stress level is dependent on the frequency of the propagated wave and the radius of the specimen. The propagation velocity being measured during the bender element test does not necessarily correspond to that of a shear wave, except within a relatively narrow range of non-dimensional frequency Ω, from 1.25 to 2.5. When Ω is greater than 8, interpreting V^* as a shear wave velocity results in a 10% underestimate of V_s. Errors up to 40% can arise if Ω of the transmitted wave is less than 1. One must carefully select the frequencies used in a bender element test so that the measured propagation velocity is representative of that of a shear wave.

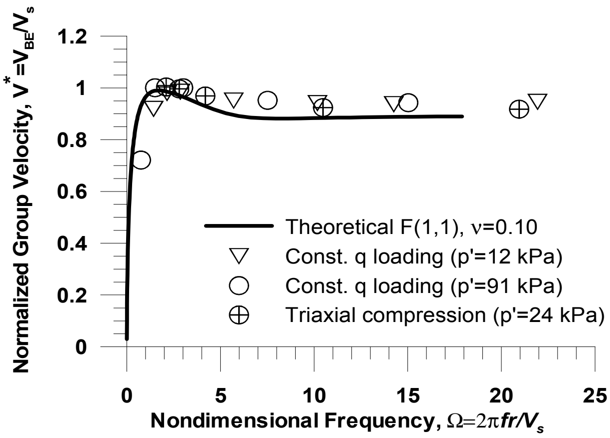

Figure 5 – Frequency-velocity dependence for bender element data

5 CONCLUSIONS

The secant shear stiffness $G_{0.001}$ has been shown to be directionally dependent at all shear strain levels between 0.001 and 0.1% for compressible Chicago glacial clay specimens obtained from block samples. The maximum secant stiffness was found to occur for a stress path direction rotated counterclockwise about 230 degrees from the initial loading history, i.e. K_0 consolidation. The results of the stress probe and bender element tests suggest that the dynamic modulus G_{BE} approximately corresponds to $G_{0.001}$ for an unloading stress path similar to a CMSE or RTE employed herein. Because bender elements induce dispersive axisymmetric flexural waves in a soil column, the frequency of the input must be carefully selected so that the measured propagation velocity is representative of a shear wave velocity.

ACKNOWLEDGMENTS

This work was supported by grant CMS-0219123 from the National Science Foundation. The authors thank Ms. Dhooli Raj of Case Foundation Co., the excavation support subcontractor, and Mr. Ron McCallister of Turner Construction Co., the general contractor at the Lurie site, for their help in obtaining the block samples.

REFERENCES

Achenbach, J.D. (1973). *Wave Propagation in Elastic Solids*. Amsterdam, North Holland.

Atkinson, J.H., Richardson, D., and Stallebrass, S.E. (1990). Effect of recent stress history on the stiffness of overconsolidated soil. *Geotechnique* **40**, No. 4, 531-540.

Chung, C.K. and Finno, R.J. (1992). Influence of depositional processes on the geotechnical parameters of Chicago glacial clays." *Engineering Geology*, 32, 225-242.

Dyvik, R., and Madshus, C. (1985). Laboratory measurements of G_{max} using bender elements. In *Advances in the Art of Testing Soils under Cyclic Conditions (edited by V. Khousla)*, Detroit, ASCE, New York, 186-196.

Finno, R.J., and Roboski, J.F. (2005). Three-dimensional response of a tied-back excavation through clay. *Journal of Geotechnical and Geoenvironmental Engineering*, ASCE, in press.

Holman, T.P. (2005). Small strain behavior of compressible Chicago glacial clays. PhD dissertation, Northwestern University.

Mayne, P. W. (2003). Personal communication.

Viggiani, G., and Atkinson, J.H. (1995). Interpretation of bender element tests. *Geotechnique*, 45(1), 149-154.

Wang, H. (2004). Theoretical evaluations of embedded plate-like and solid cylindrical concrete structures with guided waves. Ph.D. Dissertation, Northwestern University.